American Mineralogist, Volume 80, pages 998–1003, 1995

The high-pressure stability of talc and 10 Å phase: Potential storage sites for H_2O in subduction zones

ALISON R. PAWLEY,* BERNARD J. WOOD
Department of Geology, University of Bristol, Wills Memorial Building, Bristol BS8 1RJ, U.K.

ABSTRACT

The pressure-temperature conditions of the reactions governing the high-pressure stability of talc were investigated in experiments on the bulk composition $Mg_3Si_4O_{10}(OH)_2$ + H_2O at 2.9–6.8 GPa, 650–820 °C, using piston-cylinder and multianvil apparatus. The reaction talc = enstatite + coesite + vapor was bracketed between 800 and 820 °C at 2.90–2.95 GPa and between 770 and 780 °C at 3.77–4.02 GPa. The lower-pressure bracket, which is just above the quartz-coesite phase transition, is consistent with some of the previous brackets on the reaction talc = enstatite + quartz + vapor and with the position of the talc dehydration reaction calculated using THERMOCALC v2.4 (Powell and Holland, 1988; Holland and Powell, 1990; Holland, personal communication). This revised version of THERMOCALC incorporates new compressibility and thermal expansivity data for talc (Pawley, Redfern, and Wood, in preparation). Agreement between experimental and calculated curves continues up to 4 GPa, but at higher pressures the talc dehydration reaction occurs at lower temperatures than calculated, so that by 4.6 GPa the thermal stability of talc is at <730 °C. At ~5 GPa, 710 °C, there is an invariant point involving talc, 10 Å phase, enstatite, coesite, and vapor. This point marks the highest pressure at which talc is stable. Above it, the thermal stability of 10 Å phase expands with increasing pressure. Its maximum stability is unknown. Talc is a common hydrothermal alteration product of peridotite and may transport H_2O in subducting slabs from shallow depths to depths of ~150 km. It may also crystallize in overlying mantle-wedge peridotite after infiltration of fluid from the slab, and its dehydration in the mantle wedge may lead to partial melting. The 10 Å phase may transport H_2O in silica-enriched hydrated peridotite to depths of at least 200 km.

INTRODUCTION

The presence of H_2O in the Earth's mantle affects mantle properties in many ways. For example, fluid released in dehydration reactions may trigger partial melting and magma generation, and rheological and seismic properties are affected by even very small amounts of H_2O incorporated in fluids, melts, or minerals. Much of the H_2O in the mantle is introduced at subduction zones, where cold oceanic crust, hydrothermally altered at midocean ridges, is recycled back into the mantle. The principal consequence of this H_2O recycling is the abundant volcanism above descending slabs (e.g., Gill, 1981), which is the result of dehydration-melting reactions in the mantle wedge overlying the slab, involving H_2O released in dehydration reactions within the slab. It is unlikely, however, that all the H_2O present in the slab is released below arc volcanoes because some important dehydration reactions occur at greater depth. Lawsonite, for example, may be stable to depths of up to 300 km (Pawley, 1994; Schmidt and Poli, 1994) and antigorite up to 200 km (Ulmer et al., 1994). The presence of subduction-related H_2O-bearing partial melt has been suggested to be responsible for low S-wave velocity anomalies at 300–500 km depth (Nolet and Zielhuis, 1994), and it has been proposed that deep-focus earthquakes occurring at depths of up to 650 km are triggered by dehydration reactions (Meade and Jeanloz, 1991).

The above examples demonstrate the complexity of the processes of H_2O storage and release in subduction zones. Before these processes can be adequately understood, however, it is necessary to determine the stabilities of likely hydrous phases within the slab and mantle wedge and to compare the pressure-temperature positions of their dehydration reactions with models of the thermal structure of subduction zones. In this study we performed phase-equilibrium experiments to determine the stability of an important hydrous mineral, talc, and investigated the stability of its high-pressure, low-temperature hydration product, the 10 Å phase.

Talc is a common product of the hydrothermal alteration of ultramafic rocks. The extent of its occurrence depends on the bulk Mg:Si ratio, such that it is most abundant where dissolved SiO_2 has been introduced into the rock from hydrothermal solutions. Its composition

* Present address: Department of Earth Sciences, University of Manchester, Oxford Road, Manchester M13 9PL, U.K.

0003–004X/94/0910–0998$02.00

does not usually vary much from the end-member formula $Mg_3Si_4O_{10}(OH)_2$, the most common substitutions being up to about 0.15 Al replacing Si and about 0.1 Fe replacing Mg (Deer et al., 1962). H_2O contents are usually close to the ideal 4.7 wt%. Therefore, provided silicification accompanies hydration, large amounts of H_2O may be stored within talc in altered ultramafic rocks, which in subduction zones should occur in both the slab and the overlying mantle wedge. The occurrence of altered ultramafic rocks in the slab is indicated by the exposure of serpentinized peridotite on the ocean floor (e.g., Cannat, 1993) and by the presence of altered peridotite within ophiolites, and fluids released from subducting slabs should cause hydrothermal alteration of the overlying mantle wedge. Both slab and mantle wedge are expected to be considerably colder than surrounding mantle and so may retain H_2O to much greater depth. Knowledge of the stability of talc at high pressures and low temperatures is therefore important for determining the ability of hydrothermally altered ultramafic rocks to store and transport H_2O into the mantle.

Several previous experimental studies relate to the stability of talc. These have not produced consistent results. The most widely studied reaction is the dehydration reaction

$$\underset{\text{talc}}{Mg_3Si_4O_{10}(OH)_2} = \underset{\text{enstatite}}{3MgSiO_3} + \underset{\alpha\text{-quartz}}{SiO_2} + \underset{\text{vapor}}{H_2O} \quad (1)$$

which has been investigated by Chernosky et al. (1985), Kitahara et al. (1966), Jenkins et al. (1991), Wunder and Schreyer (1992), and Bose and Ganguly (1993). In these studies, temperatures of the intersection of Reaction 1 with the reaction coesite = quartz (at ~2.8 GPa) ranged from about 800 to 830 °C, and the *P-T* slope of the reaction at this pressure varied from negative to positive. The higher pressure reaction

$$\underset{\text{talc}}{Mg_3Si_4O_{10}(OH)_2} = \underset{\text{enstatite}}{3MgSiO_3} + \underset{\text{coesite}}{SiO_2} + \underset{\text{vapor}}{H_2O} \quad (2)$$

has been less extensively studied. From the results of synthesis experiments in the system MgO-SiO_2-H_2O, Yamamoto and Akimoto (1977) suggested that the thermal stability of talc decreases from 830 °C at 2.9 GPa to 740 °C at 5.5 GPa, at which point the talc stability field is pinched out because of the intersection of Reaction 2 with the reaction

$$\underset{\text{10 Å phase}}{Mg_3Si_4O_{10}(OH)_2 \cdot xH_2O} = \underset{\text{talc}}{Mg_3Si_4O_{10}(OH)_2} + \underset{\text{vapor}}{xH_2O}. \quad (3)$$

Bose and Ganguly (1993) studied Reaction 2 at pressures up to 4.5 GPa and also observed the formation of 10 Å phase at pressures above the talc stability field. However, the stability of 10 Å phase was called into question by Wunder and Schreyer (1992), who suggested that it is in fact metastable with respect to talc, in which case the maximum pressure stability of talc would not have been determined in these previous experiments.

Calculations of the *P-T* position of Reaction 2 using thermodynamic datasets (e.g., Berman, 1988; Holland and Powell, 1990) diverge considerably at high pressures, largely because of differences in the equation of state of H_2O used. These discrepancies, and the differences between the previously measured positions and slopes of Reaction 1, indicate the importance of conducting a further phase-equilibrium investigation of the high-pressure stability of talc. Our results show that Reaction 2 has a negative slope and intersects Reaction 3 at ~5 GPa, 710 °C, above which 10 Å phase is stable. These results have important implications for the stability of talc and 10 Å phase in subduction zones.

Experimental technique

The starting material for the experiments was a sample of natural talc, of ideal composition except for a 1% replacement of Mg by Fe. For most experiments a 50:50 stoichiometric mixture of talc and enstatite + quartz was used. This mixture allowed reversal experiments to be performed. The enstatite + quartz was produced by dehydrating talc at 2 GPa, 900 °C. Some experiments used enstatite + coesite, synthesized from talc at 3.2 GPa, 1000 °C, to observe the first appearance of talc, and other experiments used only talc as starting material. Excess SiO_2 in the form of coesite was added to several experiments to ensure that coesite dissolution did not lower the activity of SiO_2 in Reaction 2. The presence of quartz rather than coesite in some of the experiments was not considered significant because reaction to coesite was assumed to be faster than the rate of the talc dehydration reaction, and indeed in all the experiments quartz reacted completely to coesite. Samples were sealed in 2 mm diameter Pt capsules with ~10 wt% distilled H_2O.

For experiments at pressures up to 4 GPa an end-loaded piston-cylinder apparatus was used, with NaCl as the pressure medium. Piston-in experiments were conducted and a −0.05 GPa pressure correction applied. Quartz-coesite calibration experiments showed that a −0.05 GPa pressure correction was sufficient for piston-in experiments, and no pressure correction was necessary for piston-out experiments. The pressure uncertainty is ±0.05 GPa. Temperatures were measured using a W3Rh/W25Rh thermocouple, with no correction for pressure.

Experiments at >4 GPa were performed in the multianvil apparatus at Bristol University. This is a Walker-style apparatus (Walker et al., 1990). The anvils were 1 in. tungsten carbide cubes (Hertel) with truncated-edge lengths of 12 mm. The octahedral pressure medium was made of MgO castable ceramic (old-style Ceramacast 584, Aremco Products). $LaCrO_3$ furnaces were used (5 mm o.d., 3 mm i.d., 13 mm long) in most experiments, with stainless steel discs at both ends to provide electrical contact with the tungsten carbide cubes. The axial W3Rh/W25Rh thermocouple was placed in direct contact with the Pt capsule containing the sample, with MgO spacers and insulators around the thermocouple and capsule. Experiments were pressurized cold, and then heated while maintaining constant pressure.

TABLE 1. Results of experiments on the bulk composition $Mg_3Si_4O_{10}(OH)_2 + H_2O \pm SiO_2$

Expt.	Starting material*	*P* (GPa)	*T* (°C)	*t* (h)	Results
TA5	TEQ	2.90	800	16	Ta grew
TA3	TEQ	2.95	820	16	En + Cs grew
TA11	TEQ	3.77	770	24	Ta grew
TA16	TEQ	3.78	790	8	En + Cs grew
TA9	TEQ	3.78	800	17	En + Cs grew
TA10	TEQ	3.82	780	18	no reaction**
TA14	TEQ	4.02	780	8	En + Cs grew
TA25	TEQ	4.2	770	19	En + Cs grew
TA27†	TEQ + Cs	4.6	700	15	no reaction
TA26	TEQ	4.6	730	24	En + Cs grew
TA28†	TEQ + Cs	4.6	730	7	En + Cs grew
TA22	En + Cs	4.9	730	9	no reaction
TA23	Ta + Cs	4.9	730	12	En + Cs grew
TA24	TEQ	4.9	730	19	En + Cs grew
TA21	En + Cs	5.1	730	6	no reaction
TA19	En + Cs	5.3	730	25	no reaction
TA20	Ta + Cs	5.3	730	24	10 Å + En + Cs grew
TA15	Ta	5.6	720	9	10 Å + En + Cs grew
TA7	TEQ	5.6	750	7	10 Å + En + Cs grew
TA6	TEQ	5.6	800	19	En + Cs grew
TA12	Ta	6.8	650	44	100% 10 Å

Note: the first seven experiments are piston cylinder, the rest are multianvil. Ta = talc; En = enstatite; Cs = coesite; TEQ = stoichiometric mix of talc, enstatite, and quartz; and 10 Å = 10 Å phase.

* Ten weight percent H_2O was added to all samples except TA12, to which 15 wt% H_2O was added.

** The observation of "no reaction" in this and later experiments does not apply to the reaction of quartz to coesite, which in all experiments went to completion.

† Experiments that used a Fecralloy furnace instead of a $LaCrO_3$ furnace.

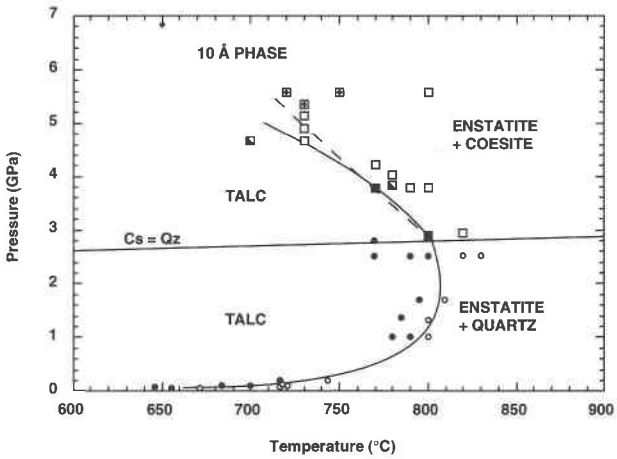

Fig. 1. Results of experiments on the bulk composition $Mg_3Si_4O_{10}(OH)_2 + H_2O$. Circles are data of Chernosky et al. (1985) and Jenkins et al. (1991); squares are from this study. Solid symbols = talc grew; open symbols = enstatite + quartz or coesite grew; half-solid symbols = no reaction. Diamonds = 10 Å phase grew. Talc = enstatite + quartz + vapor curves calculated using THERMOCALC v2.4 (Powell and Holland, 1988; Holland and Powell, 1990; Holland, personal communication) with β-quartz up to 1 GPa and α-quartz above 1 GPa. The experimental talc = enstatite + coesite + vapor curve is shown as a solid line, the calculated curve as a dashed line. Coesite = quartz is from Bohlen and Boettcher (1982).

Pressures in the multianvil apparatus were calibrated at room temperature using the Bi I-Bi II and Bi III-Bi V transitions and at high temperature using the SiO_2 quartz-coesite and $CaGeO_3$ garnet-perovskite transitions (at 2.8 GPa, 800 °C and 6.1 GPa, 1000 °C, respectively). The pressure uncertainty is ±5%, corresponding to ±0.2–0.3 GPa. The thermal gradient in the hot spot is assumed to be ≤20 °C/mm on the basis of calibrations made at 900–1500 °C using two thermocouples with no sample present (details of pressure and temperature calibrations are given in Frost and Wood, in preparation). Because separation of the thermocouple tip from the top of the sample (by Pt) is ~0.5 mm, uncertainties on quoted temperatures are assumed to be ±10 °C. At low pressures there was some difficulty achieving an electrical connection through the $LaCrO_3$ furnace, and so a furnace made of an Fe-Cr-Al alloy (Fecralloy) foil was used instead. A duplication of one of the $LaCrO_3$ experiments reproduced its result.

After each experiment, capsules were weighed, punctured, dried, and reweighed. Any that did not lose weight were discarded. The method of sample examination depended on whether the thermal gradient was small (piston-cylinder experiments) or large (multianvil experiments). In the former, all of which used the talc-enstatite-quartz starting mix, the entire sample was examined by powder XRD. A 50% change in the relative heights of the five strongest talc and enstatite peaks was taken to indicate that reaction had occurred. For the multianvil experiments, the sample closest to the thermocouple was examined optically and by XRD. The rest of the sample, at a lower temperature, was also examined, but products are not shown in Table 1 or in the figures.

RESULTS

Experimental results are listed in Table 1 and plotted in Figure 1. Experimental products comprise one to four of the phases talc, enstatite, coesite, and 10 Å phase.

Talc in the experimental products is indistinguishable from the starting-material talc; that is, it occurs as irregular plates up to 80 μm in diameter. Therefore, growth of talc in experiments on talc-enstatite-quartz mixtures could only be determined by XRD. No talc was produced in experiments on enstatite + coesite.

Enstatite forms euhedral crystals with dimensions up to 50 × 10 μm. It has straight extinction in all samples, indicating that it is orthorhombic.

Coesite was difficult to distinguish optically, but in all reversal experiments in which there was no reaction or in which enstatite grew, the presence of coesite was identified by XRD, indicating that some of it did not dissolve in the fluid.

The 10 Å phase forms euhedral hexagonal crystals up to 60 μm in diameter and 4 μm thick. Its refractive index is consistent with previous observations (n_x = 1.554, n_z = 1.574, Wunder and Schreyer, 1992). Its (001) peaks in XRD patterns are fairly broad, indicating a certain degree

of disorder, perhaps because of variable amounts of interlayer H_2O. Electron microprobe analysis indicated that it has the same Mg:Fe:Si ratio as the talc starting material, consistent with previous observations (e.g., Yamamoto and Akimoto, 1977). Previous studies have suggested various H_2O contents, e.g., expressed as $Mg_3Si_4O_{10}(OH)_2 \cdot xH_2O$, values of x of 0.65, 1, and 2 have been suggested by Wunder and Schreyer (1992), Bauer and Sclar (1981), and Yamamoto and Akimoto (1977), respectively. The first two of these values were measured in weight-loss experiments. In an experiment on a mixture of $Mg(OH)_2$ and SiO_2 with bulk composition $Mg_3Si_4O_{10}(OH)_2 \cdot 2H_2O$, we synthesized close to 100% 10 Å phase (a little talc is also present) with <1% weight loss on puncturing the capsule after the experiment and drying at 110 °C. This suggests that the estimate of x = 2 by Yamamoto and Akimoto (1977) may be correct. This value is also suggested by oxide totals obtained in electron microprobe analyses, which averaged 86.1%, close to the value of 87.0% expected for the composition $Mg_3Si_4O_{10}(OH)_2 \cdot 2H_2O$. A high H_2O content is also suggested by Fourier-transform infrared spectroscopy of 10 Å phase produced in this study. There are at least two strong OH-stretching vibrations in addition to the talc vibration at 3677 cm^{-1}. The latter has approximately the same intensity as that in spectra of talc (estimated by comparing intensities of this vibration with intensities of vibrations of the silicate framework), suggesting that the OH groups in talc are preserved on hydration to 10 Å phase. This observation contrasts with the suggestion of Bauer and Sclar (1981) that the 3677 cm^{-1} vibration is less intense in 10 Å phase than in talc.

Discussion

At 3 GPa, just above the quartz-coesite reaction, the data on Reaction 2 are consistent with the data of Jenkins et al. (1991) on Reaction 1 at 2.5 GPa. These are shown in Figure 1, together with some of the data of Chernosky et al. (1985), including data on the reaction involving β-quartz at 0.05–0.2 GPa. Because Reaction 1 has been well bracketed, it can be used to extract thermodynamic data for talc. Jenkins et al. (1991) used the brackets, together with mineral thermodynamic data from Holland and Powell (1990), to calculate the enthalpy of formation of talc, $\Delta H_{f,talc}$. However, the calculation requires knowledge of the other thermodynamic properties of talc, including its thermal expansivity and compressibility. At the time of the study of Jenkins et al. (1991), there were no published thermal expansivity data for talc, and so this had to be estimated. The compressibility data, measured in a piston-cylinder apparatus by Vaidya et al. (1973), were considered by those authors to be inaccurate. Therefore, the calculated value of $\Delta H_{f,talc}$ was subject to some uncertainty. To allow the calculation to be refined and reactions involving talc to be calculated to higher pressures and temperatures, the thermal expansivity of talc was recently measured and the compressibility remeasured (Pawley, Redfern, and Wood, in preparation). The compressibility of 10 Å phase was also measured. Thermal expansivity data were obtained by using powder X-ray diffraction to determine cell parameters of the sample heated in air, and the compressibility was measured using synchrotron radiation, with the sample compressed in a diamond-anvil cell. The thermal expansivity of talc is described by the equation $V/V_0 = 1 + 2.15\ (\pm 0.05) \times 10^{-5}\ (T - 298)$, where V_0 = 136.52 (±0.03) cm^3/mol. The isothermal bulk modulus, K, and its pressure derivative, K', were obtained by fitting the compressibility data to the Murnaghan equation, $V/V_0 = [1 + (K'/K)P]^{-1/K'}$. For talc, K = 41.6 ± 0.9 GPa and K' = 6.5 ± 0.4. For 10 Å phase, K = 32.2 ± 5.5 GPa and K' = 9.2 ± 2.8. The talc data have been incorporated by Holland and Powell in their latest version of THERMOCALC (version 2.4, Holland, personal communication), in which thermal expansivities are represented by the equation $\alpha = \alpha_0 - 10\alpha_0 T^{-1/2}$ and compressibilities by the Murnaghan equation with K' = 4. The revised value of $\Delta H_{f,talc}$ in the dataset is −5891 kJ/mol. The position of Reaction 1 calculated using THERMOCALC v2.4 is shown in Figure 1. It reaches a maximum temperature of 807 °C at 1.9 GPa.

Reaction 2 is bracketed to lie between 800 and 820 °C at 2.90–2.95 GPa and between 770 and 780 °C at 3.77–4.02 GPa. These brackets are in good agreement with its position calculated using THERMOCALC v2.4, but at higher pressures the experimental curve bends back to lower temperatures than the calculated curve. The experimental curve (solid line in Fig. 1) follows the calculated curve (dashed line) to 4 GPa and then decreases in slope to pass below 4.6 GPa, 730 °C, where talc reacted to enstatite + coesite + vapor. The divergence between calculated and experimental curves is not great, considering the uncertainties involved, namely the multianvil pressure uncertainty of ±0.2 GPa and temperature uncertainty of ±10 °C, and uncertainties in the thermodynamic data used in the calculation.

At high pressures, Reaction 3, 10 Å phase = talc + vapor, was encountered. In the experiments at 5.3–5.6 GPa, 720–750 °C, with talc in the starting material, 10 Å phase was produced, and enstatite + coesite grew. The 10 Å phase cannot be in equilibrium with enstatite + coesite in a pressure-temperature field with H_2O in excess and so must represent metastable crystallization from talc within the enstatite + coesite + vapor field. Therefore, the metastable extension of Reaction 3 was crossed, and the samples lie on the high-temperature side of the reaction

$$10\ \text{Å phase} = \text{enstatite} + \text{coesite} + \text{vapor}. \quad (4)$$

Presumably, with longer experimental durations enstatite + coesite would increase at the expense of 10 Å phase in this field. The absence of 10 Å phase crystallizing from talc at 4.9 GPa, 730 °C and 5.6 GPa, 800 °C, suggests that these points lie below Reaction 3. Because there was no 10 Å phase in any of the starting material, Reaction 3 was not reversed and could lie at a lower pressure than the pressure conditions of its synthesis.

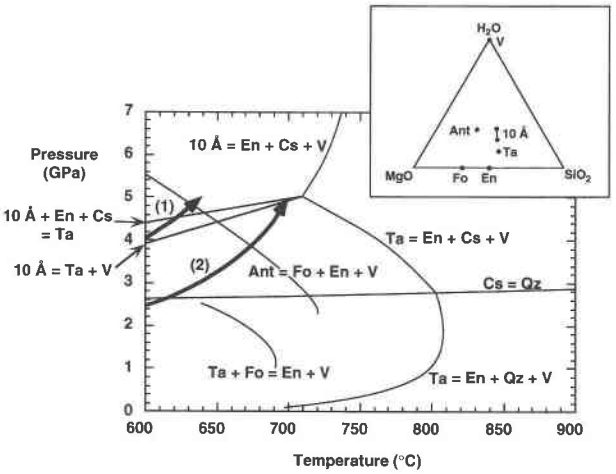

Fig. 2. Summary of experimental data in the system MgO-SiO_2-H_2O for bulk compositions with Mg:Si < 2. Reactions are from Fig. 1, plus talc + forsterite = enstatite + vapor from Guggenbuehl (1994), antigorite = forsterite + enstatite + vapor from Ulmer et al. (1994), and 10 Å phase = talc + vapor, 10 Å phase + enstatite + coesite = talc, and 10 Å phase = enstatite + coesite + vapor estimated from the results of this study. All reactions are given with the low-temperature phases on the left side. Curves labeled (1) and (2) are *P-T* paths for the top of subducting oceanic crust converging at 10 cm/yr, with a brittle-ductile transition at 300 and 500 °C, respectively (Peacock et al., 1994). Inset shows compositions of phases. The 10 Å phase is shown with 2–3 H_2O per formula unit.

At 6.8 GPa, 650 °C, a sample of talc + H_2O reacted completely to 10 Å phase over a period of 44 h. The long duration and absence of enstatite in the experimental product suggests that these conditions are within the field of stable 10 Å phase, i.e., on the low-temperature side of Reaction 4. Although the position of Reaction 4 is very poorly constrained, its slope can be estimated by calculating the volume change for the reaction. The $\Delta V_{\text{Reaction 4}}$ was calculated at 5 GPa, 710 °C, the approximate position of the invariant point involving Reactions 2, 3, and 4. Assuming that the thermal expansivity of 10 Å phase is the same as that of talc, and that 10 Å phase has two H_2O p.f.u. (Bauer and Sclar, 1981), $\Delta V_{\text{Reaction 4}} \approx 2.1$ cm³/mol (calculated using volume data from THERMOCALC v2.4; cf. $\Delta V_{\text{Reaction 2}} \approx -1.5$ cm³/mol). If 10 Å phase has three H_2O p.f.u. (Yamamoto and Akimoto, 1977), $\Delta V_{\text{Reaction 4}} \approx 3.4$ cm³/mol. Being a dehydration reaction, $\Delta S_{\text{Reaction 4}}$ is probably positive, and therefore dP/dT ($= \Delta S/\Delta V$) is positive. Therefore, in contrast to the behavior of talc, the stability field of 10 Å phase expands with increasing pressure above 5 GPa.

Implications for H_2O recycling in subduction zones

Our results on the stability of talc and 10 Å phase are compared in Figure 2 with other recent phase equilibrium data relevant to the stability of hydrous phases in altered peridotite in subduction zones. Also shown are parts of two *P-T* paths calculated for the tops of subducting slabs in mature subduction zones (Peacock et al., 1994). These calculations assume that shear heating in the slab is not important at temperatures above a brittle-ductile transition, and therefore lead to steep *P-T* paths. The subduction rate is 10 cm/yr, and the brittle-ductile transition occurs at 300 and 500 °C for the paths labeled (1) and (2), respectively. Temperatures are higher for slower subduction rates, higher brittle-ductile transition temperatures, and subduction of younger oceanic crust. They are also higher for mantle-wedge material, and so dehydration of talc in mantle-wedge peridotite at 3–4 GPa could be partly responsible for triggering partial melting and arc magmatism. On the other hand, temperatures decrease with depth in the slab, so the temperature at the base of a 7.5 km thick basaltic crust is ~200 °C lower than at the top of the crust (Peacock, 1990). Therefore, the stabilities of talc to 5 GPa and 10 Å phase to >6.8 GPa indicate that H_2O may be transported in SiO_2-rich compositions in subduction zones to a depth of at least 200 km.

The occurrence of the reaction talc + forsterite = enstatite + vapor at a much lower pressure and temperature than Reaction 2 (Guggenbuehl, 1994) shows that for bulk compositions on the MgO-rich side of the enstatite-H_2O join (inset to Fig. 2), i.e., typical mantle compositions, talc stability is greatly reduced. The higher pressure part of this reaction is in fact metastable because it occurs within the stability field of antigorite (Ulmer et al., 1994). So for these bulk compositions, antigorite is the main hydrous phase until the *P-T* path crosses the reaction antigorite = forsterite + enstatite + vapor. Thereafter, talc can be present only if the bulk composition lies to the SiO_2-rich side of the enstatite-H_2O join. Solution reprecipitation of SiO_2 during seafloor alteration may produce large volumes of silica-rich compositions in the oceanic crust (as well as silica-depleted regions). With increasing pressure the solubility of SiO_2 in H_2O increases (Manning, 1994), and so SiO_2-metasomatism in subducting slab and overlying mantle wedge may be widespread and lead to more extensive talc crystallization.

When the stability field of 10 Å phase is entered, 10 Å phase should crystallize from talc through either Reaction 3, talc + vapor = 10 Å phase, or the reaction talc = 10 Å phase + enstatite + coesite, depending on whether excess vapor is present. The approximate positions of these reactions are shown in Figure 2, as is Reaction 4, 10 Å phase = enstatite + coesite + vapor, which passes through 7 GPa at >730 °C and is expected to extend to higher temperatures with increasing pressure. The maximum pressure stability of 10 Å phase is unknown, and therefore the fate of H_2O incorporated in 10 Å phase in subduction zones can only be conjectured. It may be that *P-T* paths passing through its stability field cross Reaction 4, causing H_2O to be liberated, or they may cross a different, as yet unknown, high-pressure breakdown reaction. In either case, the stability of 10 Å phase could determine the maximum depth to which H_2O is sub-

ducted in SiO_2-enriched peridotites, making this phase an important one for further study related to H_2O recycling in subduction zones.

Acknowledgments

Financial support for this study was provided by NERC grant GR3/8362. We thank Tim Holland for providing the updated version of THERMOCALC, Evgeny Wassermann for useful discussions, and Jianzhong Zhang for a helpful review of the manuscript.

References cited

Bauer, J.F., and Sclar, C.B. (1981) The "10 Å phase" in the system MgO-SiO_2-H_2O. American Mineralogist, 66, 576–585.

Berman, R.G. (1988) Internally consistent thermodynamic data for minerals in the system Na_2O-K_2O-CaO-MgO-FeO-Fe_2O_3-Al_2O_3-SiO_2-TiO_2-H_2O-CO_2. Journal of Petrology, 29, 445–522.

Bohlen, S.R., and Boettcher, A.L. (1982) The quartz = coesite transformation: A precise determination and the effects of other components. Journal of Geophysical Research, 87, 7073–7078.

Bose, K., and Ganguly, J. (1993) Stability of talc at high pressures: Experimental determination, retrieval of thermodynamic properties, and applications to subduction processes. Geological Society of America Abstracts with Programs, 25, 213–214.

Cannat, M. (1993) Emplacement of mantle rocks in the seafloor at mid-ocean ridges. Journal of Geophysical Research, 98, 4163–4172.

Chernosky, J.V., Jr., Day, H.W., and Caruso, L.J. (1985) Equilibria in the system MgO-SiO_2-H_2O: Experimental determination of the stability of Mg-anthophyllite. American Mineralogist, 70, 223–236.

Deer, W.A., Howie, R.A., and Zussmann, J. (1962) Rock-forming minerals, vol. 3: Sheet silicates, 270 p. Longmans, London.

Gill, J. (1981) Orogenic andesites and plate tectonics, 390 p. Springer-Verlag, New York.

Guggenbuehl, E. (1994) Stabilität von Talk, Forsterit und Enstatit im Feld und Experiment. Diploma thesis, University of Zurich, Zurich, Switzerland.

Holland, T.J.B., and Powell, R. (1990) An enlarged and updated internally consistent thermodynamic dataset with uncertainties and correlations: The system K_2O-Na_2O-CaO-MgO-MnO-FeO-Fe_2O_3-Al_2O_3-TiO_2-SiO_2-C-H_2-O_2. Journal of Metamorphic Geology, 8, 89–124.

Jenkins, D.M., Holland, T.J.B., and Clare, A.K. (1991) Experimental determination of the pressure-temperature stability field and thermochemical properties of synthetic tremolite. American Mineralogist, 76, 458–469.

Kitahara, S., Takenouchi, S., and Kennedy, G.C. (1966) Phase relations in the system MgO-SiO_2-H_2O at high temperatures and pressures. American Journal of Science, 264, 223–233.

Manning, C.E. (1994) The solubility of quartz in H_2O in the lower crust and upper mantle. Geochimica et Cosmochimica Acta, 58, 4831–4839.

Meade, C., and Jeanloz, R. (1991) Deep-focus earthquakes and recycling of water into the Earth's mantle. Science, 252, 68–72.

Nolet, G., and Zielhuis, A. (1994) Low S velocities under the Tornquist-Teisseyre zone: Evidence for water injection into the transition zone. Journal of Geophysical Research, 99, 15813–15820.

Pawley, A.R. (1994) The pressure and temperature stability limits of lawsonite: Implications for H_2O recycling in subduction zones. Contributions to Mineralogy and Petrology, 118, 99–108.

Peacock, S.M. (1990) Fluid processes in subduction zones. Science, 248, 329–337.

Peacock, S.M., Rushmer, T., and Thompson, A.B. (1994) Partial melting of subducting oceanic crust. Earth and Planetary Science Letters, 121, 227–244.

Powell, R., and Holland, T.J.B. (1988) An internally consistent thermodynamic dataset with uncertainties and correlations: 3. Applications to geobarometry, worked examples and a computer program. Journal of Metamorphic Geology, 6, 173–204.

Schmidt, M.W., and Poli, S. (1994) The stability of lawsonite and zoisite at high pressures: Experiments in CASH to 92 kbar and implications for the presence of hydrous phases in subducted lithosphere. Earth and Planetary Science Letters, 124, 105–118.

Ulmer, P., Trommsdorff, V., and Reusser, E. (1994) Experimental investigation of antigorite stability to 80 kbar. Mineralogical Magazine, 58A, 918–919.

Vaidya, S.N., Bailey, S., Pasternick, T., and Kennedy, G.C. (1973) Compressibility of fifteen minerals to 45 kilobars. Journal of Geophysical Research, 78, 6893–6898.

Walker, D., Carpenter, M.A., and Hitch, C.M. (1990) Some simplifications to multianvil devices for high pressure experiments. American Mineralogist, 75, 1020–1028.

Wunder, B., and Schreyer, W. (1992) Metastability of the 10-Å phase in the system MgO-SiO_2-H_2O (MSH): What about hydrous MSH phases in subduction zones? Journal of Petrology, 33, 877–889.

Yamamoto, K., and Akimoto, S. (1977) The system MgO-SiO_2-H_2O at high pressures and temperatures—Stability field for hydroxyl-chondrodite, hydroxyl-clinohumite and 10 Å-phase. American Journal of Science, 277, 288–312.

Manuscript received January 20, 1995
Manuscript accepted May 4, 1995